Article

Protein analysis of *A. halleri* and *N. caerulescens* hyperaccumulators when exposed to nano and ionic forms of Cd and Zn.

Valentina Gallo[1], Valentina M. Serianni[1], Davide Imperiale[1,2], Andrea Zappettini[4], Marco Villani[4], Marta Marmiroli [1*], and Nelson Marmiroli [4]

[1] Department of Chemistry, Life Sciences and Environmental Sustainability, University of Parma, 4 Parma, Italy; valentina.gallo@unipr.it; marta.marmiroli@unipr.it; valentina.serianni@uochb.cas.cz

[2] Experimental Station for the Food Preservation Industry –Research Foundation, Parma, Italy; davide.imperiale@ssica.it

[3] Institute of Materials for Electronics and Magnetism (IMEM), National Research Council (CNR), 6 Parma, Italy; andrea.zappettini@imem.cnr.it; marco.villani@imem.cnr.it

[4] The Italian National Interuniversity Consortium for Environmental Sciences (CINSA), Parma, Italy; nelson.marmiroli@unipr.it;

* Correspondence: marta.marmiroli@unipr.it; Tel.: +39 0521 905698

Abstract: Hyperaccumulator plant species growing on metal-rich soils can accumulate high quantity of metals and metalloids in aerial tissues and several proteomic studies on the molecular mechanisms at the basis of metals resistance and hyperaccumulation have been published. Hyperaccumulator are also at the basis of phytoremediation strategy to remove more efficiently metals from polluted soils or water. *Arabidopsis halleri* and *Noccea caerulescens* are both hyperaccumulators of metals and nano-metals. In this study it was assessed the change in some proteins in *A. halleri* and *N. caerulescens* after the growth in soil with cadmium and zinc, provided as sulphate salts (CdSO$_4$ and ZnSO$_4$) or sulfide quantum dots (CdS QDs and ZnS QDs). The protein extracts obtained from plants after 30 days of growth were analyzed by 2D-gel electrophoresis (2D SDS-PAGE) and identified by MALDI-TOF/TOF mass spectrometry. A bioinformatics analysis was carried out on quantitative protein differences between control and treated plants. In total, 43 proteins resulted significatively modulated in *A. halleri*, while 61 resulted modulated in *N. caerulescens*. Though these two plants are hyperaccumulator of both metals and nano-metals, at protein levels the mechanisms involved do not proceed in the same way but at the end bring to a similar physiological result.

Keywords: Proteomics; 2D SDS-PAGE; Nanoscale and ionic metals; Quantum dots; Hyperaccumulator

1. Introduction

One groups of nanoparticles extensively exploited for their biomedical and industrial applications are Quantum dots (QDs). A characteristic of the Quantum dots is a metal core composed of cadmium (Cd), tellurium (Te), arsenic (As), lead (Pb), zinc (Zn), copper (Cu), or selenium (Se), alone or in combination [1]. Use of engineered QDs is advantageous because they have a small size, regular crystal shape, a large surface area to mass ratio and possess strong affinity to metals thus reducing their availability for plant in metal-rich soil. Plants in natural environments are constantly exposed to a combination of biotic and abiotic stress [2]. Drought, salinity, water logging, heat, cold, metals, UV radiation are hurdles which plants face at some degree of their life cycle [3]. In agricultural soils, an excessive level of metals can reduce soil quality, crop yield and compromise the integrity of agricultural products, as well as cause possible hazard to humans, animals and ecosystem health. On metal-rich soil, certain plant species and varieties have evolved and adopted toxic metals as common minerals [4]. Metal hyperaccumulators have developed an exclusive strategy to achieve tolerance by diverting the largest amount of metal into

the aerial parts, stems and leaves with the formation of complex coordination bound either with 0 or S which makes these complex less toxic [5].

Hyperaccumulator plants could become a resource for phytoremediation of metals [6,7], to extract metals from soil and concentrate in their upper parts. Several species of the *Brassicaceae* family are metal hyperaccumulators [8], and studies have suggested an evolutionary role of hyperaccumulation as a defense against the herbivores [9] and pests [10]. *Noccaea caerulescens* (J. Presl & C. Presl) F.K. Mey. (former *Thalaspi caerulescen*) and *Arabidopsis halleri* (L.) O'Kane & Al-Shehbaz, have been model plants in metal hyperaccumulation [7, 11], largely because of their genetic analogy with the model species *Arabidopsis thaliana* (L.) Heynh and because their genomes have 94% and 88.5% correspondence in coding regions respectively [12]. *N. caerulescens* is a Zn and Cd hyperaccumulator and accumulates these metals at concentrations exceeding 1% of shoot dry biomass; but Cd seems to be less consistently hyperaccumulated than Zn [13]. Similarly, *A. halleri* is a known Cd hyperaccumulator but also a Zn hyperaccumulator [14]. The capacity that some *Brasicacee* family members have for storing large amounts of divalent cations in their vacuoles might explain why this families comprises about 50% of all know metal hyperaccumulation plant taxa (about 400 specie) [15]. Whereas hyperaccumulators are "competitive" in presence of high metal they do not suffer particular disadvantages when the environment conditions are non-selective, showing a large degree of phenotypic plasticity [16]. A way to understand the plasticity of the hyperaccumulator phenotype were considering the interaction between gene and environment at protein level. A proteomic approach can show which proteins were involved in response to metal -based NMs like QDs. Recently it was suggested that cases of environmental dispersion of NMs could be treated with plant as in phytoremediation of metals [17]. Here we suggest that QDs phytoremediation can benefit from the knowledges emerging from proteomic study of two hyperaccumulator models: *A. halleri* and *N. caerulescens* in term of functions and genes useful for implementing the technology.

2. Materials and Methods

The ZnS QDs and CdS QDs (uncoated) were synthesized by CNR-IMEM (Parma, Italy) following the methods of Villani *et al.,* (2012) [18]. The CdS QDs have a bulk density of 4.82 g cm^{-3} and an average diameter of 5 nm. Cd represents 78% of the dry weight of the QD; the Z-potential for these nanoparticles was +61.6 mV and they have a hydrodynamic range of 1190 nm. The ZnS QDs had an average diameter under 5 nm, with Zn representing 63% of the dry weight of each QD. The ZnS QDs have a Z-potential of +34.9 mV and a hydrodynamic range of 248.7 nm. Details of the synthesis and characterization are provided in Imperiale *et al.* (2022) [19].

2.2 Growth condition and Treatments

Seeds of *A. halleri* Langhelsheim were kindly provided by Prof. S. Clemens (Department of Plant Physiology, University of Bayreuth, Germany). Seeds of *N. cearulescens* Monte Prinzera accession were taken from our collection from the Monte Prinzera site (Fornovo, Parma, Italy), a serpentine hill near Parma, Italy. One seed of *A. halleri* and *N. caerulescens* was placed in each pot and was germinated in a growth chamber (MIR-554-PE, Panasonic, Osaka, Japan) for 72 h at 25 °C, under a relative humidity of 50% and dark conditions. After germination, pots with seedlings were transferred to a greenhouse with average temperatures of 25/16 °C (day/night), and light supplemented by a metal halide lamps to maintain a minimum light intensity of 300 μmol m^{-2} s^{-1}, with a 14 h photoperiod. According to their growth cycles, plants were grown for different periods prior to treatment: 60 days for *A. halleri* and 45 days for *N. caerulescens*. The watering frequency was 30 ml of deionized water, twice a week. After growth, plants were treated: *A. halleri* with 10 mg of Cd administered as CdSO$_4$ and CdS QDs and *N. caerulescens* with 10 mg of Zn administered as ZnSO$_4$ and ZnS QDs; three biological replicates for condition (Figure S1 and S2).

The plants were maintained for additional 30 days under the same conditions of temperature, humidity, light and irrigation. One gram of the aerial part of plant material was collected for each condition, gently washed with distilled H_2O, frozen in liquid nitrogen and then stored at –80°C for the following proteomic analysis. The controls (untreated) were prepared in the same way. The experiment was conducted in triplicate.

2.3 Proteins extraction and separation with two-dimensional gel electrophoresis (2D SDS-PAGE)

Total proteins were extracted from leaves of *A. halleri* and *N. caerulescens*, grown under the experimental conditions previously described (Figure S1 and S2). The proteins extraction was performed with a phenol-based buffer as described in Gallo *et al.,* (2021) [20]. Protein's concentration was evaluated according to a modified Bradford assay based on the acidification of the sample [21] buffer with 20 mM HCl. Bovine serum albumin (BSA) was used as standard.

The selected pH gradient must compose all pI of proteins in the mixture and allow the best separation for maximal resolution of gels. In this case, the strip with 5-8 pH range was selected for *A. halleri* and the strip with 3-10 pH range was selected *for N. caerulescens* because it allowed the detection of the larger number of spots and was used throught out for all samples. For proteins separation in the first dimension, 300 μg of total proteins from each sample were loaded onto 11-cm ReadyStrip pH 5-8 and 3-10 IPG strips (BioRad, USA) which had been rehydrated overnight with 250 μL IEF buffer containing the sample. Proteins were focused by using the PROTEAN® i12™ IEF System (BioRad, USA) following this program: 250 V (60 min), 1000 V (60 min), 8000 V (2 hours) to reach 8000 V for a total of 35000 V/h. After IEF, the strips were incubated 15 min in 3 ml of reducing buffer containing 2% w/v DTT, 6 M Urea, 0.375 M Tris-HCl (pH 8.8), 20% w/v glycerol, 2% w/v SDS and for 15 min in 3 ml of alkylating buffer containing 2.5% w/v iodoacetamide, 6 M Urea, 0.375 M Tris-HCl (pH 8.8), 2% w/v glycerol. The second dimension (SDS-PAGE) was performed using a CriterionTM Dodeca™ cell (BioRad, USA) and 12% Criterion™ XT Bis-Tris gels (BioRad, USA) in 1 M MOPS (3-(N-morpholino)-propanesulfonic acid) buffer containing 1 M Tris, 20 mM EDTA and 2% w/v SDS.

2D- gels were stained with QC Colloidal Coomassie G-250 (BioRad, USA) and gel images were obtained with a ChemiDocTM Imaging System (BioRad, USA). Image analysis was performed using the PDQuest software (BioRad, USA). Spots detection and matching between gels were performed automatically, followed by manual verification. The spots densities were normalized by local regression method and subsequently against the whole gel densities. The percentage density of each spot was averaged over three replicates gels and Student's t-test analysis (p<0.05) was performed to find out statistically significant differences in proteins abundance. Statistically relevant spots were successively excised from the gels using an EXQuest Spot Cutter (BioRad, USA), distained by soaking the pieces of acrylamide for 30 min in a 1:1 solution of 100 mM ammonium bicarbonate and acetonitrile, and the proteins were hydrolysed with trypsin following the Shevchenko *et al.,*(2006) protocol [22].

2.4 Protein identification and data mining

Tryptic peptides were desalted and concentrated to a final volume of 4 μl with Zip-Tip C18 (Millipore Corporation, Billerica, MA, USA), according to the manufacturer's protocol, then dispersed into an α-cyano-4-hydroxycinnamic acid (4-HCCA) matrix, prepared by dissolving 4-HCCA in 50% acetonitrile/0.05% trifluoroacetic acid and spotted on a MALDI plate. The samples were subjected to analysis through a model 4800 MALDI-TOF/TOFTM MS analyzer (Applied Biosystems, Foster City, CA, USA). Peptide mass fingerprint (PMF) were acquired in reflectron mode (500-4000 m/z range) and analyzed with the help of mMass v5.5 open-source software (http://www.mmass.org/). For each feature,

a peak list was created and then manually checked for the presence of signal from the matrix complex, trypsin and human keratin peptides. PMF analysis was carried out with the software Mascot (http://www.matrixscience.com) and proteins were identified by searching off for confidence of match in   Swiss-Prot database (Swiss-Prot Viridiplantae taxonomic subdatabase of 'nr'nonredundant) database of the UniProtKB-Swissprot,

2.5 Statistical analysis, Data mining and bioinformatic analysis

Venn diagrams were constructed using the software Venny 2.1 program (Oliveros, J.C., 2007-2015, Venny http://bioinfogp.cnb.csic.es/tools/venny/index.html). The Gene Ontology analysis was performed through the Panther database (pantherdb.org/). Classification of proteins was performed using MapMan software (http://mapman.ga-bipd.org/mapman-download) based on *A. thaliana* genome database and the results were manually verified using the annotations of UniProt database. MapMan was used to place proteins within a likely pathway (BIN).   Heat maps of selected proteins were generated by R v3.3.1 (www.r-project.org).

3. Results

3.1 Differential proteomic analysis: comparison between plants and treatments

After acquisition by Bio-Rad's PDQuest 2-D analysis software, the gels were analyzed. A number of 206 and 180 spots were sufficiently clear to be appreciated in *A. halleri* and *N. caerulescens* respectively. The next step was comparing the spots intensities through comparative pairwise protein analysis between control, treated sample with QDs (CdS QDs and ZnS QDs) and treated sample with salts (CdSO$_4$ and ZnSO$_4$). Spots whose intensity resulted statistically significant using the *t-Student* test were considered (values below the threshold 0,05 were considered significant) and a number of 43 for *A. halleri* and 61 for *N. caerulescens* significative spots were identified whose intensities increased or decreased during the treatments (Figure 1). For *A. halleri* the number of spots with significantly increased or decreased intensity are reported in Figure 1A as a Venn diagrams. Among these 43 spots: 30 of these had an identification from the comparison between control and treatment with CdS QDs. The spots up-regulated with the treatment with CdS QDs were 12, while those down-regulated with the same treatment were 18. Comparison between control and treatment with CdSO4 has identified 17 spots statistically significant. The spots up-regulated were 3, while those down-regulated were 14 (Figure 1A).   Spots shared among pairwise comparisons corresponded to proteins up or down regulated in the two different conditions and were highlighted by the intersections in the Venn Diagrams (Figure 1A). The spots shared between CdSO4 down and CdS QDs down were 4 (DNA repair protein recA homolog 2, Pentatricopeptide repeat-containing protein At1g28690, Transcription factor KAN4, Ras-related protein RABE1d) (Figure 1A) all down regulated.

Similarity, among the 61 spots of *N. caerulescens*: 42 of these were identified from the comparison of control and treatment with ZnS QDs, and 36 from the comparison between control and treatment with ZnSO4 (Figure 1B).   Among the 42 spots: 23 were up-regulated, while those down-regulated were 19. From the treatment with Zn, among the 36 spots: 17 were up-regulated, while those down-regulated were 19. Spots shared among pairwise comparisons corresponded to proteins up or down regulated in the two treatments and were highlighted by the intersections of the Venn Diagrams (Figure 1B). The spot shared between ZnS QDs down and ZnSO4 down is 1 (Alpha-1,6-mannosyl-glyco-protein 2-beta-N-acetylglucosaminyltransferase) whereas the spots shared between ZnS QDs up and ZnSO4 up were 7(30S ribosomal protein S19 chloroplastic, 3-ketoacyl-CoA synthase 12, Cytochrome b-c1 complex subunit 7-2, Jasmonate O-methyltransferase, Protein trichome birefringence-like 6, Ras-related protein RABA1c, tRNA-splicing

endonuclease subunit Sen2-1). There are also spots with opposite behavior (up or down-regulated) compared to the treatments: the spots shared between ZnSO4 up and ZnS QDs down were 7 (2S seed storage protein 4, Late embryogenesis abundant protein 46, NADH dehydrogenase [ubiquinone] 1 beta subcomplex subunit 7, Nascent polypeptide-associated complex subunit beta, NDR1/HIN1-like protein 26, Serine carboxypeptidase-like 52, Thioredoxin F-type chloroplastic) whereas the spots shared between ZnSO4 down and ZnS QDs up were 2 (Defensin-like protein 39, and E3 ubiquitin-protein ligase PRT1) (Figure 1B).
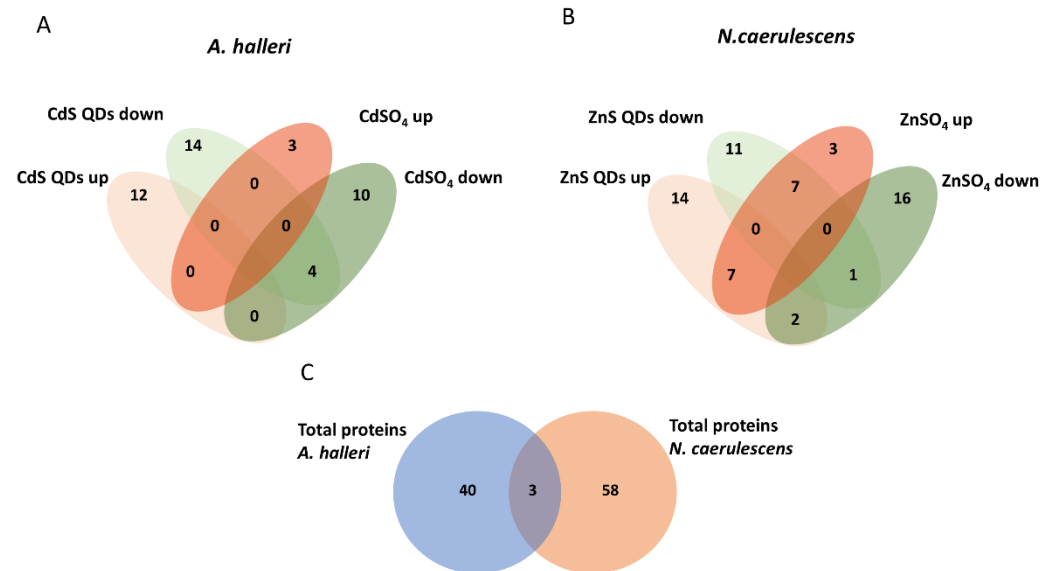
Figure 1. Representation of the effect of exposure to Cd (CdS QDs or CdSO$_4$) and Zn (ZnS QDs or ZnSO$_4$) on proteome. The Venn Diagrams stands for up and down-regulated proteins treated with Cd in *A. halleri*: **(A)** and treated with Zn in *N. caerulescens* **(B)**. In **(C)** proteins in common between two hyperaccumulators are numerated.

Proteins identified through comparative pairwise among three conditions in two types of plants, were indicated in the tables (Table S1 and S2). From the comparison of the two set of proteins isolated and identified from two hyperaccumulators it was evident only a limited overlapping. In fact, there were only 3 proteins commonly modulated in the two hyperaccumulators (Figure 1C): ATP synthase delta chain (Atpd), Ribulose bisphosphate carboxylase large chain (rbcl), and F-box protein (At3g18320).

A heat map was used for a graphical representation of the protein abundance in treatments as compared to control, through the "R" software (*R Project for Statistical Computing*). The binary logarithm of the spots color intensities ratio between a treated sample and control was used to generate the heat map, consequently in the graphical representation, the values are represented by different shade of colors green and red. The columns represent two different treatments while the rows represent the identified proteins, considered for the comparison (Figure 2, 3). In *A. halleri*, Atpd resulted up regulated in the treatment with QDs and down regulated in the treatment with Cd salt, while in *N. caerulescens* resulted down regulated in both treatments. In *A. halleri* Rbcl resulted down regulated in both treatments, while in *N. caerulescens* resulted up regulated in the treatment with QDs and down regulated in the treatment with Zn salt. In *A. halleri* At3g18320 resulted up regulated in the treatment with QDs and down regulated in the treatment with salt, while in *N. caerulescens* resulted down regulated in both the treatments (Figure 2, 3).
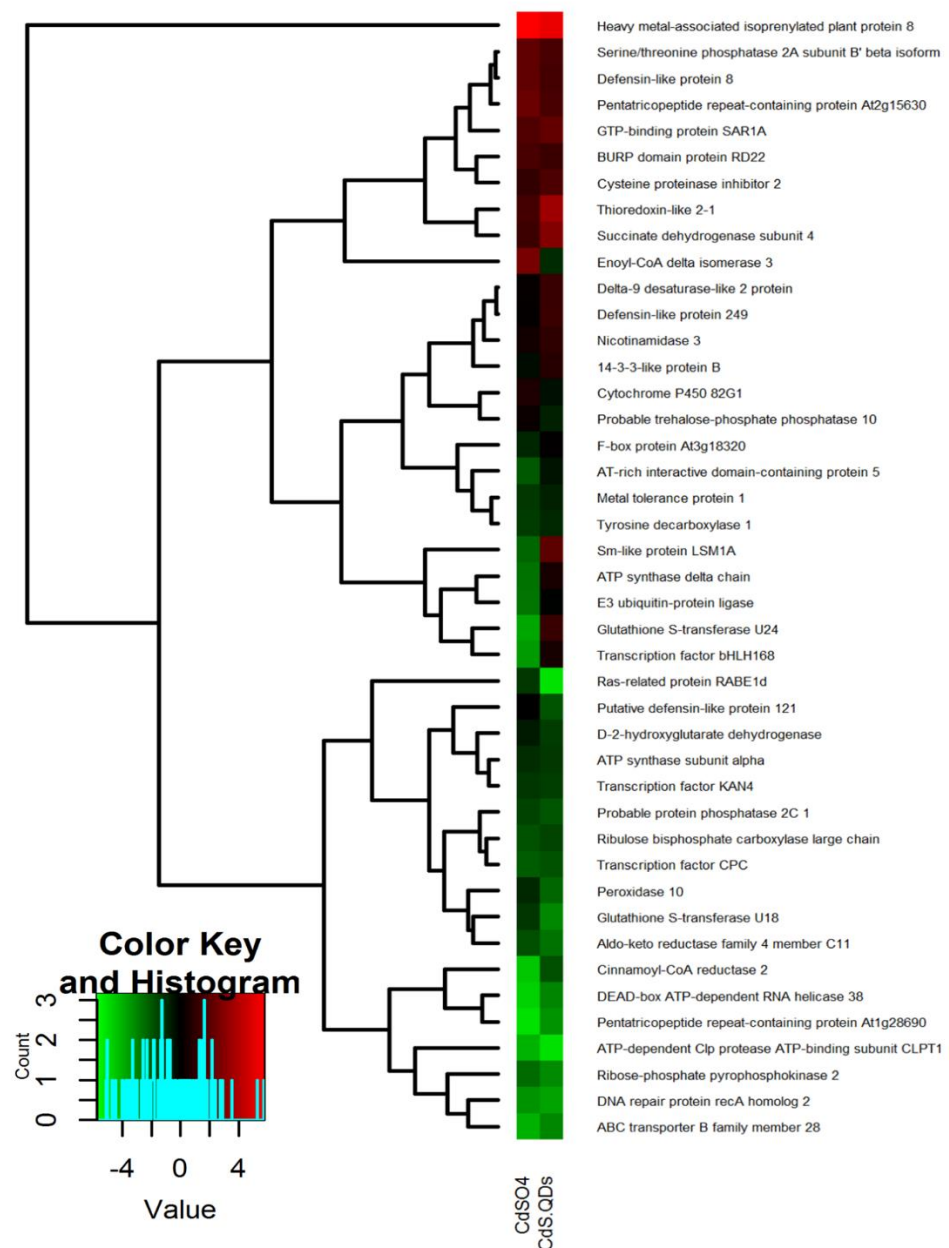
Figure 2. Heat map of proteins of *A. halleri* identified after separation by 2D SDS-PAGE and obtained through the "R" software. The columns represent two different treatments while the rows represent the identified proteins. Shade of reds indicates high abundance of proteins and shade of green indicates low abundance of proteins in the treated samples as compared to the control which therefore is not shown here. In particular, the first column represents the abundance of proteins in the treated samples with CdSO$_4$ and the second column represents the abundance of proteins in the treated samples with CdS QDs. The heat map was assembled by cluster analysis therefore similar levels of expression in treatments as compared to the control are positioned at short distance, while different levels of expression in treatments as compared to the control are positioned at long distance. The more abundant proteins in treated samples compared to the control are positioned at the top, the less abundant proteins are positioned at the bottom. Proteins that have an opposite behavior in the treated samples and in the control are positioned in the center of the figure.
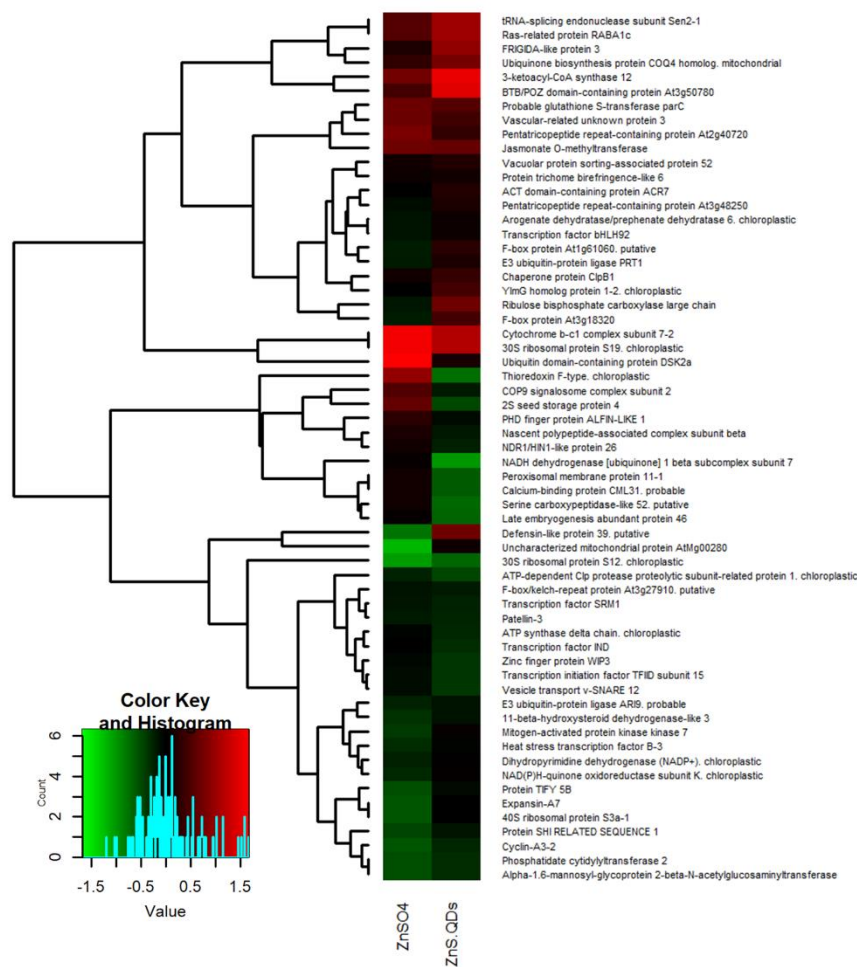
Figure 3. Heat map of proteins of *N. caerulescens* identified after separation by 2D SDS-PAGE and obtained through the "R" software. The columns represent two different treatments while the rows represent the identified proteins. Shade of reds indicates high abundance of proteins and shade of green indicates low abundance of proteins in the treated samples as compared to the control which therefore is not shown here. In particular, the first column represents the abundance of proteins in the treated samples with ZnSO₄ and the second column represents the abundance of proteins in the treated samples with ZnS QDs. The heat map was assembled by cluster analysis therefore similar levels of expression in treatments as compared to the control are positioned at short distance, while different levels of expression in treatments as compared to the control are positioned at long distance. The more abundant proteins in treated samples compared to the control are positioned at the top, the less abundant proteins are positioned at the bottom. Proteins that have an opposite behavior in the treated samples and in the control are positioned in the center of the figure.

3.2 Gene ontology analysis

PANTHER database (Protein ANalysis THrough Evolutionary Relationships) was used for the Gene Ontology analysis. Using information about genome sequencing of other plant organisms, three independent ontologies were used to define complete information for each inserted gene and to describe genic product: Molecular function, Biological process and Cellular component. For *A. halleri* the list of genes inserted in the software were 30 genes obtained from the comparative analysis between control and treated with CdS QDs and 17 genes obtained from the comparative analysis between control and treated

with CdSO₄. For *N. caerulescens* the list of genes inserted in the software were: 42 genes obtained from the comparison between control and treatment with ZnS QDs, and 36 from the comparison between control and treatment with ZnSO₄. In figure 3,4 and 5, are represented the commons and uncommon molecular functions, biological processes and cellular component in the two hyperaccumulators.

For molecular functions the most represented class in the two comparisons was the catalytic activity (Figure 4). The common molecular functions in the comparison between Ctrl *vs* QDs were catalytic activity, binding, transporter activity, and ATP-dependent activity. The exclusive class of *N. caerulescens* were molecular adaptor activity, and structural molecule activity (Figure 4A). The common classes in the comparison between Ctrl *vs* salt were: catalytic activity, transporter activity, transcription regulator activity, and binding, while the exclusive class of *N. caerulescens* were molecular function regulator, and structural molecule activity (Figure 4B).
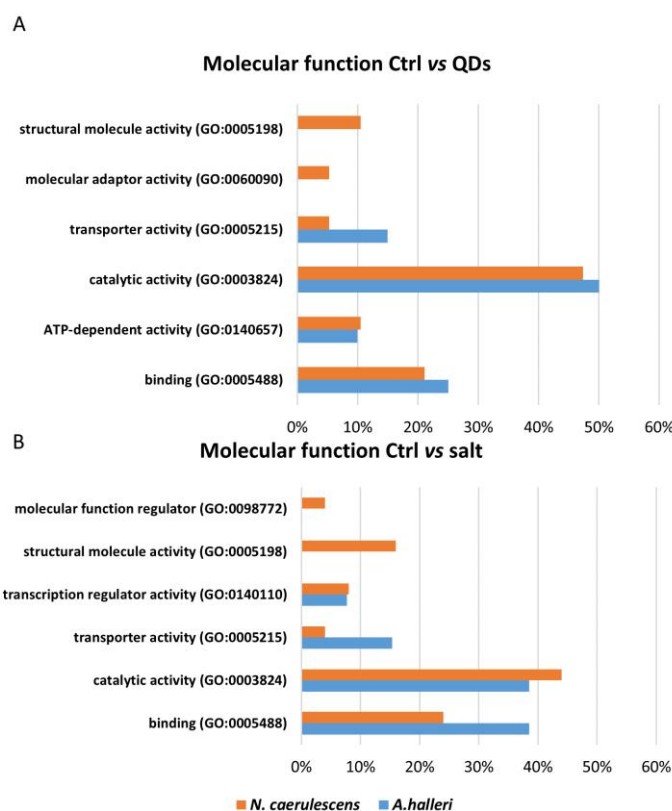

Figure 4. The GO analysis of Molecular Function. The genes list inserted are genes that code for proteins identified using comparative pairwise proteomic analysis between control, treated with metal QDs and metal salt. Blue bars represent the percentage of the proteins, found in *A. halleri*, while orange bars represent the percentage of the proteins, found in *N. caerulescens*.

The percentage of genes that coded for proteins that have a specific biological function, involving multiple molecular functions, are reported in two different diagrams (Figure 5). In these diagrams, the most represented class, in the two comparisons, was cellular process. The common represented classes in a comparison between Ctrl *vs* QDs were: cellular process, metabolic process, localization, biological regulation and developmental process. The exclusive classes of *N. caerulescens* were growth and response to stimulus (Figure 5A). The common classes in a comparison between Ctrl *vs* salt were cellular process, metabolic

process, biological regulation, and localization. The exclusive class of *A. halleri* was biological process involved in interspecies interaction between organisms and growth.
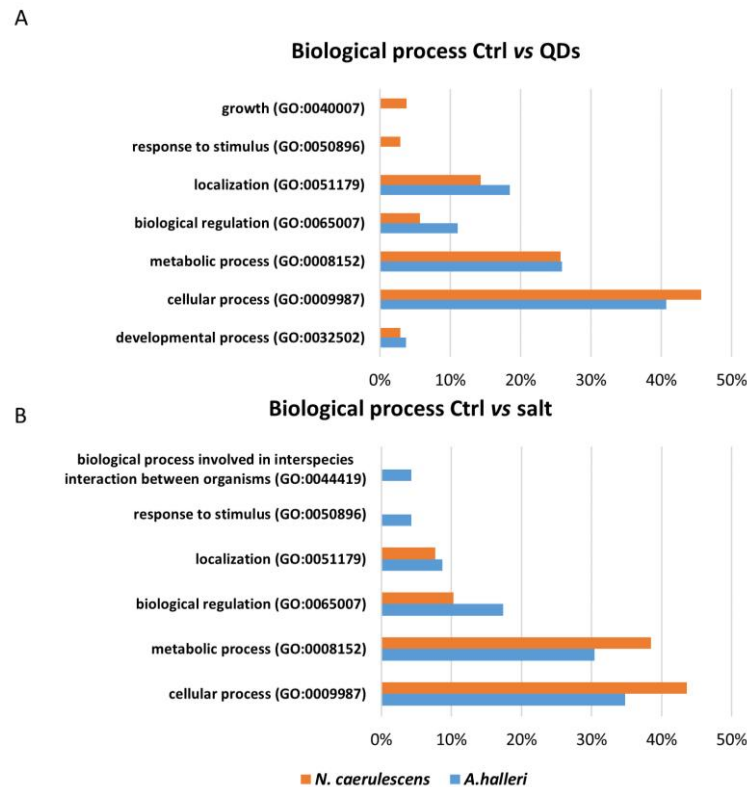

Figure 5. The GO analysis of Biological process. The genes list inserted are genes that code for proteins identified using comparative pairwise proteomic analysis between control, treated with metal QDs and metal salt. Blue bars represent the percentage of the proteins, found in *A. halleri*, while orange bars represent the percentage of the proteins, found in *N. caerulescens.*

The percentage of genes that coded for proteins that have a specific localization at the subcellular level or in macromolecular complexes, are reported in figure 6 (Figure 6). The common classes in the comparison between Ctrl *vs* QDs were: intracellular anatomical structure, cytoplasm, membrane, organelle, organelle subcompartment, endomembrane system, protein containing complex, intracellular anatomical structure, cytosol, and cell periphery. The exclusive classes of *A. halleri* were supermolecular complex, and endoplasmic reticulum site. (Figure 6A). The common classes in the comparison between Ctrl *vs* salt were: organelle, protein containing complex, cell periphery, intracellular anatomical structure, membrane, and cytoplasm. The exclusive class of *N. caerulescens* was endomembrane system, while the exclusive class of *A. halleri* was supermolecular complex (Figure 6B).

A

Cellular component Ctrl *vs* QDs

B

Cellular component Ctrl *vs* salt
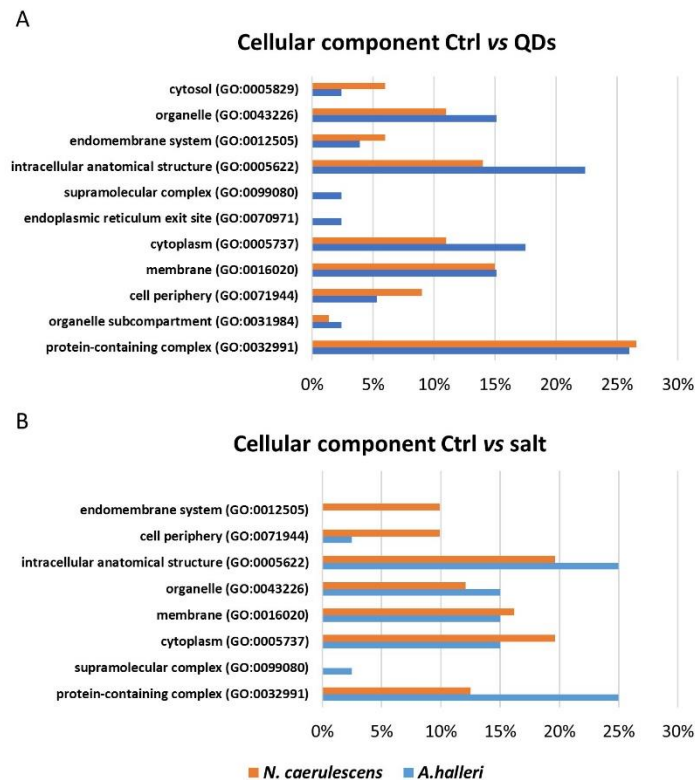
■ *N. caerulescens*   ■ *A.halleri*

Figure 6. The GO analysis of Cellular component. The genes list inserted are genes that code for proteins identified using comparative pairwise proteomic analysis between control, treated with metal QDs and metal salt. Blue bars represent the percentage of the proteins, found in *A. halleri*, while orange bars represent the percentage of the proteins, found in *N. caerulescens*.

3.3 Pathway analysis

Metabolic pathway analysis was performed by submitting the Gene IDs of the proteins identified in two different plants to the MapMan server (http://www.gomapman.org) for *A. thaliana* to identify the pathways that were more represented. For all the proteins, the MapMan ontology BIN assignations are listed in Table S3 for *A. halleri* and in Table S4 for *N. caerulescens*. In *A. halleri*, the set of reprogrammed proteins were associated with the following major MapMan bins: RNA regulation of transcription, protein degradation, protein post-transcriptional modification, abiotic and biotic stress, lipid metabolism, redox ascorbate and glutathione biosynthesis. (Figure 7). In *N. caerulescens*, the set of reprogrammed proteins was associated with protein degradation, protein synthesis, RNA regulation of transcription, abiotic and biotic stress, photosynthesis and photorespiration, signaling, and mitochondrial electron transport and ATP synthesis (Figure 7). This last pathway, together with amino acid metabolism, cell and development, are exclusive of *N. caerulescens*, while DNA synthesis is exclusive of *A. halleri*.
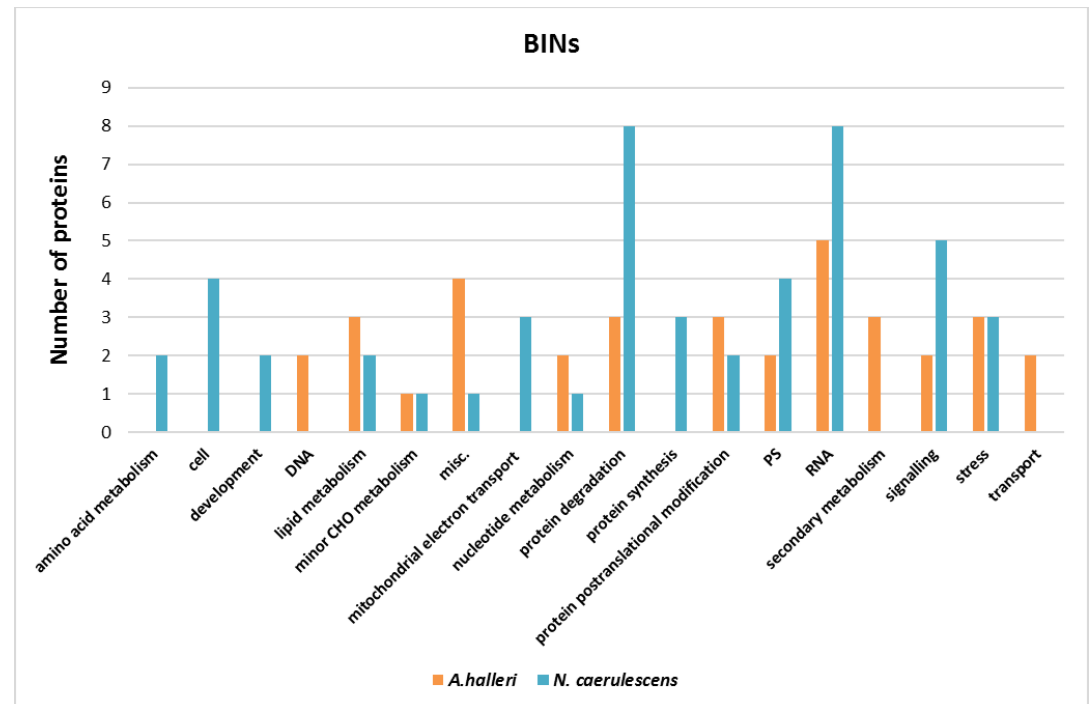
Figure 7. Responsive proteins according to MapMan ontology. The distribution of responsive proteins in *A. halleri* (in blue) and of *N. caerulescens* (in orange) according to MapMan ontology classification (BINs). On the x axis there are the different MapMan bins types, on the y axis are the number of proteins for each bin.

4. Discussion

The study of the hyperaccumulators *A. halleri* and *N. caerulescens* suggests that when the plants were treated with 10 mg of Cd or Zn in the nano form (CdS or ZnS QDs) or as salt ($CdSO_4$ or $ZnSO_4$), the response can be quite similar at morphological and physiological levels [7]. The characterization of protein response to treatments with Cd or Zn in nanoscale or ionic form, due to the low number of proteins resolved by the 2D-gel cannot be considered a throughout proteomic analysis [20] because of the throughput of the method. But this approach was used instead of performing transcriptomic analysis because of the higher relatedness that proteins molecules had to gene expression and to plant phenotype. On the other hand, for the proteomic analysis it was chosen the 2D SDS- PAGE technique because of its simplicity and considering also that the number and the intensities of the spots differentially abundant in control and treatments were well evident considering their relative's high amount. Moreover, 2D SDS-PAGE is a 'top-down' proteomics method that analyzes intact proteins directly, by preserving their post-translationally modified forms displayed *in vivo* without any previous proteolytic digestion [23]. As a prototypical 'top-down' proteomics technique, the 2D gel-based proteomics have relevant applications [24, 25]. Although this technique has some advantages, as possibility to identify post-translational modified (PTM) proteins and protein isoforms, it has also significant limitations [26]. The application here of this comparative analysis has allowed to be identifying the spots with intensity values statistically significant. The spots shared between treatments in the pairwise comparisons were displayed in a Venn Diagram as in the figure 1. The spots relevant from a biological point of view were then identified by MS and assigned to a specific molecular function, metabolic pathway and cellular component. The two different pIs used for the first dimension gel in the two hyperaccumulators respected the separation patterns that we observed at all pH ranges tested. The range between the two were 5-8 for *A. halleri* and 3-10 for *N. caerulescens*.

4.1 Proteomic analysis of differentially expressed proteins in A. halleri

A. halleri after the treatments with ionic or nanoforms Cd showed some specific proteomic features (Figure 2) as the downregulation of the ABC transporter protein (Abcb28), involved in the transport of metals in the vacuole and in other cellular structures [27]. The stress induced by nanomaterial treatment has decreased the presence of proteins with antioxidant activity: aldo-keto reductase (Akr4c11), glutathione S-transferase (Gstu18), peroxidase (Per10), cinnamoyl-CoA reductase 2 (Ccr2). Particularly, GSTs, were involved both in detoxification and in hyperaccumulation of Cd [28] and it was modulated both in the control and in the treated samples. However, the behavior of glutathione S-transferase (Gstu24) was opposite in the treatment with CdS QDs as compared to treatments with CdSO4, as highlighted in the heat map, whereas the other oxidoreductases were down regulated after the two treatments (Figure 2). Two transcription factors were down regulated by the treatments: transcription factor CPC (Cpc) and KAN4 (Kan4) (Figure 2). The first is expressed in trichomes and in young developing leaves, it represses trichome development by lateral inhibition [29]; the second regulates carpel integuments formation by modulating the content of flavonols and proanthocyanidin in seeds [30].

On the contrary, the gene for heavy metal-associated isoprenylated plant protein 8 (Hipp08), was up regulated in both treatments (Figure 2). Hipp08 is a metallochaperone protein for the safe transport of metallic ions inside the cell [31]. HIPPs may be involved in heavy metal homeostasis and detoxification, particularly concerning cadmium tolerance, transcriptional responses to cold and drought, and plant-pathogen interactions [31]. The list of the proteins identified in the comparative analysis was used to obtain the GO analysis. In the molecular function bar chart, the "ATP-dependent activity" class was under expressed in the comparison between Ctrl *vs* CdS QDs (Figure 4A). It is evident that the treatment with CdS QDs determines the modulation, up or down, of proteins involved in oxidative phosphorylation. In fact, Gallo *et al.*, (2020) [32] demonstrated that CdS QDs treatments caused a reduction in oxidative phosphorylation and in ATP production in yeast. Moreover, some proteins, involved in the energy production, ATP synthase subunit alpha (Atp1) and ATP-dependent Clp protease ATP-binding (Clpt1), were down regulated (Figure 2). Farinati and colleagues indicated a general upregulation of photosynthesis-related proteins in *A. halleri* exposed to metals Cd and Zn, and to metals plus microorganisms, suggesting that metal accumulation in shoots is an energy-demanding process [33]. In the biological process bar chart there were two classes, represented in the comparison between Ctrl *vs* salt, which were absent in the comparison between Ctrl *vs* QDs response to stimulus and biological process involved in interspecies interaction between organisms, while one class, development process, was present in   Ctrl *vs* QDs and was absent in Ctrl *vs* salt (Figure 5A). The proteins identified in these classes were Transcription factor CPC and Cytochrome P450 82G1. Some of this class proteins, not necessarily those identify here, could also be involved in "biotransformation" of nanoparticles which takes place after nanoparticles internalization [34]. In the class biological regulation, in Ctrl *vs* QDs, belong three proteins: GTP-binding protein Sar 1a, Thioredoxin-like 2-1 and Transcription factor KAN4. Sar 1a plays a key role in the control of vesicle transport and could be involved in the cellular transport of nanoparticles [35]. This protein was up regulated in both treatments. (Figure 2). Thioredoxin-like 2-1 is an oxidoreductase that may participate in various redox reactions and some assays of subcellular localization demonstrated that this protein is localized to the chloroplast [36]. In the cellular components bar chart (Figure 6A), the membrane class emerge when comparing Ctrl *vs* QDs. Delta-9 desaturase-like 2 protein (At1g06100), D-2-hydroxyglutarate dehydrogenase (D2hgdh) and ABC transporter B family member 28 (Abcb28) were among the more interesting. Abcb28 is involved in the transport of metals toward the vacuole or other cellular structures [37]; At1g06100 is involved in the polyunsaturated fatty acid biosynthesis [38] and was up regulated in both treatments. Some membrane proteins indeed could be over-produced in the presence of nanoform of Cd as well as in the presence of ionic Cd.

4.2 *Analysis of differentially expressed proteins in N. caerulescens*

Similarly to *A. halleri*, also in *N. caerulescens* after the treatments, the most affected proteins were involved in oxidative stress. In this case, the comparison concerned Ctrl, nano Zn and ionic Zn. Probable glutathione S-transferase parC (ParC) was up regulated in both treatments, Peroxisomal membrane protein 11-1(Pex11-1) was down regulated in the treatment with QDs and up regulated in the treatment with salt, and E3 ubiquitin-protein ligase (Ari9) was down regulated in both treatments (Figure 3). Four transcription factors were down-regulated by the treatments: transcription factor SRM1 (Srm1), transcription initiation factor TFIID subunit 15 (Taf15), heat stress transcription factor B-3(Hsfb3) and transcription factor IND (Ind) (Figure 3). A down regulation of these transcription factors suggests that there could have been an inhibition of transcription due to the treatments. In particular, the presence of the transcription regulator activity class in GO analysis is also highlighted (Figure 4B). Concerning GO analysis, in the molecular function bar chart, the ATP-dependent activity class is shown in the comparison Ctrl *vs* QDs (Figure 4A). Two proteins involved in energy production, ATP synthase delta chain chloroplastic (Atpd) and ATP-dependent Clp protease proteolytic subunit-related protein 1 chloroplastic (Clpr1), were down regulated (Figure 3) as reported for *A. halleri.* These two proteins were localized together in the chloroplast, and previous studies in *A. thaliana* treated with QDs highlighted the role of chloroplast as a potential target of the ENMs [39, 20]. Moreover, the mutation in a gene encoding for a protein of chloroplast function lead to resistance to QDs [40]. Clpr1was required for chloroplast development and differentiation [41]. Atpd is an ATP synthase which produces ATP from ADP in the presence of a proton or sodium gradient and is essential for photosynthesis, by facilitating electron transport in both photosystems I and II [42]. Wang *et al.,* (2016) showed that CuO NPs impedes electron transport between the two photosystems which can cause an increase of ROS and generation of oxidative stress, damaging biological molecules and disrupting cellular metabolism [43].

4.3 *Pathway analysis*

Mapman ontology, allowed the identification of several common pathways particularly involved in the response to nano or ionic form of Cd and Zn. Many proteins belong to RNA regulation of transcription bin. Interestingly, in *N. caerulescens* two proteins, Protein SHI related sequence 1(Srs1) and Zinc finger WIP3 (Wip3), which belong at zinc family transcription factor (TF) family. Srs1 is a transcription activator and promotes auxin homeostasis by regulating gene expression as well as genes affecting stamen development, cell expansion and timing of flowering [44]. Synergistically with other SHI-related proteins, regulates gynoecium, stamen and leaf development in a dose-dependent manner, controlling apical-basal patterning, promotes stilo and stigma formation and influences vascular development during gynoecium development [44]. This effect which can extend its influence on flower development was also observed and described in Zucchini [34]. Wip3 belongs to WIP proteins, a plant specific subfamily of C_2H_2 zinc finger (ZF) proteins, and work in order to coordinate zinc ions to maintain characteristic tertiary of the protein structures [45]. These two proteins, Srs1 and Wip3, were down regulated after both treatments (Figure 3). Another important TF was Hsfb3 which belongs to heat stress transcription factors (Hsfs) family. Hsfs are the terminal components of a signal transduction chain mediating the activation of genes responsive to both heat stress and to chemical stressors [46]. In *A. halleri* were identified proteins involved in regulation of transcription, as the AT-rich interactive domain-containing protein 5 (Arid5), Transcription factor CPC (Cpc) and Transcription factor Kan4 (Kan4).

Recent papers show that treatment with ENMs increase or decrease functionality of the organelles in *A. thaliana* [40, 47]. In fact, in chloroplasts the common protein ATP synthase delta chain (Atpd) in *A. halleri* was down regulated in the treatment with $CdSO_4$ and up

regulated in the treatment with QDs, whereas in *N. caerulescens* it was down regulated after both treatments. This same protein had a different behavior in the two hyperaccumulators. Moreover, the same protein NAD(P)H-quinone oxidoreductase subunit K, localized in the chloroplast, was up regulated after treatment with QDs and down regulated after treatment with $ZnSO_4$. In *N. caerulescens* there are three proteins that are part of the mitochondrial electron transport and ATP synthesis pathway: Ubiquinone biosynthesis protein COQ4 homolog (COQ4), and Cytochrome b-c1 complex subunit 7-2 (QCR7-2) and NADH dehydrogenase [ubiquinone] 1 beta subcomplex subunit 7 (At2g02050). The first two proteins were up regulated after both treatments, while At2g02050 was down regulated in the treatment with QDs and up regulated in the treatment with $ZnSO_4$ (Figure 3). Conversely in *A. halleri* no proteins belonging to this pathway showed a particular regulation after treatments.

4.4 Comparison between the two hyperaccumulators and A. thaliana

To make a comparison intra species with *A. thaliana* treated with CdS QDs we took advantage of a similar study performed in *A. thaliana* [20]. A comparison of the three set of proteins identified: in the two hyperaccumulators and in *A. thaliana* showed only a limited overlapping. In fact, there was only 1 protein modulated in common among the three: the Ribulose bisphosphate carboxylase large chain (rbcl); while in common between *A. thaliana* and *N. caerulescens* there was also tRNA-splicing endonuclease subunit Sen2-1 (Sen1). Sen1 is located in the nucleus and constitutes one of the two catalytic subunits of the tRNA-splicing endonuclease complex, a complex responsible for identification and cleavage of the splicing sites in pre-tRNA [48]. Furthermore, comparing the proteins modulated in the two hyperaccumulators with another work on *A. thaliana* treated with CdS QDs, but where the proteins were separated by 2D-liquid chromatography (LC) with ProteomeLab™ PF2D (Beckman) [49], we find other commonly modulated proteins. We found 2 proteins in common with *A. halleri*: Glutathione S-transferase U24 (Gstu24) and Putative defensin-like protein 121(Lcr55). While in common with *N. caerulescens* we found 3 proteins: Arogenate dehydratase/prephenate dehydratase 6, chloroplastic (Adt6), Calcium-binding protein CML31, (Cmlr31) and E3 ubiquitin-protein ligase ARI9 (Ari 9).

Comparing three types of plants of the same Brassicaceae family, one nonmetal hyperaccumulator and two hyperaccumulators, with a low throughput but reliable methodology 2D SDS-PAGE, the total number of proteins modulated in *A. thaliana* [20] was larger than in the two hyperaccumulators (98 *vs* 43 and 61). Therefore, the regulative response of *A. thaliana* was stronger than in the two hyperaccumulators in response to Cd or Zn. For example, the pathways, mitochondrial electron transport and ATP synthesis, hormone metabolism, abiotic and biotic stress, and redox ascorbate and glutathione biosynthesis, were barely present or totally absent in the two hyperaccumulators. This may be related with the fact that the two hyperaccumulators resist better to exposure as reported in Imperiale *et al.* (2022) [7] and do not need an extensive remodeling of gene expression; they are substantially "tolerant" to the metals in nano or ionic form.

5. Conclusions

In conclusion, the gene regulation at the level of proteins produced in both hyperaccumulators was differentially affected by exposure to ionic or nano forms of Cd or Zn. Also, in the hyperaccumulator plants, metal uptake, transport and accumulation of metals inside plant are energy-demanding processes, and here there was a confirmation of this in the general modulation of photosynthesis-related proteins observed also in Farinati *et al.*, (2009) [33]. In fact, several proteins regulated by exposure belong to *ATP-dependent activity* in GO analysis. Another pathway and group of proteins, regulated in the two hyperaccumulators, are those related to ROS production, with stream response and with chaperoning of damaged proteins. The final conclusion concerns the difference between ionic and

nano -metals, both Cd and Zn. This was already shown at phenotypic level [7], but it is confirmed here at protein level. The mechanism of hyperaccumulation certainly extend from ionic to nano metals, as well the mechanism of resistance [32]. But the mechanism of tolerance rests on different proteins and functions, not excluding those that lead to a bio-transformation of the nano-form once inside the plant [34].

Author Contributions: Conceptualization M.M. and N.M.; methodology V.G., V.S. and, D.I.; validation V.G., V.S. and, D.I.; writing original draft preparation, V.G., M.M. and N.M. writing—review and editing M.M. and N.M.; M.V. and A.Z. provided the QDs and their physico-chemical characterization.   All authors have read and agreed to the published version of the manuscript.

Data Availability Statement: Not applicable

Conflicts of Interest: The authors declare no conflict of interest.

References

1. Gleiter, H. Nanostructured Materials: Basic Concepts and Microstructure. *Acta Mater.* **2000**, *48*, 1–29,

2. Singh, S. and Husen A. Role of Nanomaterials in the Mitigation of Abiotic Stress in Plants. In *Nanomaterials and Plant Potential* Springer Nature Switzerland AG. **2019,** Volume 18, pp. 441-471.

3. Manzoor, N.; Ali, L.; Ahmed, T.; Noman, M.; Adrees, M.; Shahid, M.S.; Ogunyemi, S.O.; Radwan, K.S.A.; Wang, G.; Zaki, H.E.M. Recent Advancements and Development in Nano-Enabled Agriculture for Improving Abiotic Stress Tolerance in Plants. *Front. Plant Sci.* **2022**, *13*, 1–12.

4. Mustafa, G.; Komatsu, S. Toxicity of Heavy Metals and Metal-Containing Nanoparticles on Plants. *Biochim. Biophys. Acta - Proteins Proteomics* **2016**, *1864*, 932–944.

5. Marmiroli, M.; Lepore, G.O.; Pagano, L.; d'Acapito, F.; Gianoncelli, A.; Villani, M.; Lazzarini, L.; White, J.C.; Marmiroli, N. The fate of CdS Quantum Dots in plants as revealed by Extended X-ray Absorption fine structure (EXAFS) analysis. *Environ. Sci. Nano.* **2020**, *7*, 1150-1162.

6. Suman, J.; Uhlik, O.; Viktorova, J.; Macek, T. Phytoextraction of Heavy Metals: A Promising Tool for Clean-up of Polluted Environment? *Front. Plant Sci.* **2018**, *871*, 1–15.

7. Imperiale, D.; Lencioni, G.; Marmiroli, M.; Zappettini, A.; White, J.C.; Marmiroli, N. Interaction of hyperaccumulating plants with Zn and Cd nanoparticles. *Science of the Total Environment* **2022,** 817, 152741

8. Krämer, U. Metal Hyperaccumulation in Plants. *Annu. Rev. Plant Biol.* **2010**, *61*, 517–534

9. Behemer, S. T.; Lloyd, C. M.; Raubenheimer, D.; Stewart- Clark, J.; Knight, J., Leighton, R. S.; Harper F. A.; Smith J. A. C. Metal hyperaccumulation in plants: mechanisms of defence against insect herbivores. *Functional Ecology* **2005**, *19*, 55 – 66

10. Fones, H; Davis, C. A. R.; Rico, A.; Fang, F.; Smith, J. A. C.; Preston, G. M. Metal Hyperaccumulation Armors Plants against Disease. *Plos Pathog.* **2010**, *6*(9).

11. Assunção, A.G.L.; Schat, H.; Aarts, M.G.M. Thlaspi Caerulescens, an Attractive Model Species to Study Heavy Metal Hyperaccumulation in Plants. *New Phytol.* **2003**, *159*, 351–360.

12. Rigola, D.; Fiers, M.; Vurro, E.; Aarts, M.G.M. The Heavy Metal Hyperaccumulator Thlaspi Caerulescens Expresses Many Species-Specific Genes, as Identified by Comparative Expressed Sequence Tag Analysis. *New Phytol.* **2006**, *170*, 753–766.

13. Reeves, R.D.; Schwartz, C.; Morel, J.L.; Edmondson, J. Distribution and Metal-Accumulating Behavior of Thlaspi Caerulescens and Associated Metallophytes in France. *Int. J. Phytoremediation* **2001**, *3*, 145–172.

14. Shanmugam, V.; Lo, J.C.; Yeh, K.C. Control of Zn Uptake in Arabidopsis Halleri: A Balance between Zn and Fe. *Front. Plant Sci.* **2013**, *4*, 1–5.

15. van der Ent, A.; Baker, A.J.M.; Reeves, R.D.; Pollard, A.J.; Schat, H. Hyperaccumulators of Metal and Metalloid Trace Elements: Facts and Fiction. *Plant Soil* **2013**, *362*, 319–334.

16. Visioli, G.; Marmiroli, N. The Proteomics of Heavy Metal Hyperaccumulation by Plants. *J. Proteomics* **2013**, *79*, 133–145.

17. Sarma, H.; Narayanc, M.; Peralta-Videac, J-R.; Lam, S.S. Exploring the significance of nanomaterials and organic amendments — Prospect for phytoremediation of contaminated agroecosystem. *Environmental Pollution* **2022,** 30811960.

18. Villani, M., Calestani, D., Lazzarini, L., Zanotti, L., Mosca R., Zappettini, A. Extended functionality of ZnO nanotetrapods by solution-based coupling with CdS nanoparticles. *J. Mater. Chem.* **2012**, *22*, 5694.

19. Imperiale, D.; Lencioni, G.; Marmiroli, M.; Paesano, L.; Zappettini, A.; White, J.C.; Marmiroli, N. Data on the Interaction of Hyperaccumulating Plants with Nanoscale Metals Zn and Cd. *Data Br.* **2022**, *42*, 108171.

20. Gallo, V.; Zappettini, A.; Villani, M.; Marmiroli, N.; Marmiroli, M. Comparative analysis of proteins regulated during cadmium sulfide Quantum Dots response in Arabidopsis thaliana wild type and tolerant mutants. *Nanomaterials* **2021**, *11*, 615.

21. Ramagli, L.S.; Rodriguez, L. V. Quantitation of Microgram Amounts of Protein in Two-dimensional Polyacrylamide Gel Electrophoresis Sample Buffer. *Electrophoresis* **1985**, *6*, 559–563.

22. Shevchenko, A.; Tomas, H.; Havliš, J.; Olsen, J. V.; Mann, M. In-Gel Digestion for Mass Spectrometric Characterization of Proteins and Proteomes. *Nat. Protoc.* **2007**, *1*, 2856–2860.

23. Siuti, N.; and Kelleher N.L. Decoding protein modifications using top-down massspectrometry. *Nat Methods*. **2007,** *4*, 817–821

24. Huang, Z.; Ma, L.; Huang, C.; Li, Q.; Nice, E.C. Proteomic Profiling of Human Plasma for Cancer Biomarker Discovery. *Proteomics* **2017**, *17*, 1–13.

25. Carberry, S.; Ohlendieck, K. Gel Electrophoresis-Based Proteomics of Senescent Tissues. *Methods Mol. Biol.* **2013**, *1048*, 229–246.

26. Zhang, Y.; Fonslow, B.R.; Shan, B.; Baek, M-C.; Yates, J.R. Protein Analysis by Shotgun/Bottom-up Proteomics. *Chem. Rev.* **2013**, *113*, 2343−23942345

27. Sánchez-Fernández, R.; Davies, T.G.E.; Coleman, J.O.D.; Rea, P.A. The Arabidopsis Thaliana ABC Protein Superfamily, a Complete Inventory. *J. Biol. Chem.* **2001**, *276*, 30231–30244.

28. Dixon, D.P.; Skipsey, M.; Edwards, R. Roles for Glutathione Transferases in Plant Secondary Metabolism. *Phytochemistry* **2010**, *71*, 338–350.

29. Schellmann, S.; Schnittger, A.; Kirik, V.; Wada, T.; Okada, K.; Beerman, A.; Thumfahrt, J.; Jürgens, G.; Hülskamp, M. TRIPTYCHON and CAPRICE Mediate Lateral Inhibition during Trichome and Root Hair Patterning in Arabidopsis. *EMBO J.* **2002**, *21*, 5036–5046.

30. Gao, P.; Li, X.; Cui, D.; Wu, L.; Parkin, I.; Gruber, M.Y. A New Dominant Arabidopsis Transparent Testa Mutant, Sk21-D, and Modulation of Seed Flavonoid Biosynthesis by KAN4. *Plant Biotechnol. J.* **2010**, *8*, 979–993.

31. De Abreu-Neto, J.B.; Turchetto-Zolet, A.C.; De Oliveira, L.F.V.; Bodanese Zanettini, M.H.; Margis-Pinheiro, M. Heavy Metal-Associated Isoprenylated Plant Protein (HIPP): Characterization of a Family of Proteins Exclusive to Plants. *FEBS J.* **2013**, *280*, 1604–1616.

32. Gallo, V.; Srivastava, V.; Bulone, V.; Zappettini, A.; Villani, M.; Marmiroli, N.; Marmiroli, M. Proteomic analysis identifies markers of exposure to Cadmium Sulphide Quantum Dots (CdS QDs). Nanomaterials **2020**, 10, 1214.

33. Farinati, S.; Dal Corso, G.; Bona, E.; Corbella, M.; Lampis, S; Cecconi, D.; Polati, R.; Berta, G.; Vallini,G.; Furini, S.; Proteomic analysis of Arabidopsis halleri shoots in response to the heavy metals cadmium and zinc and rhizosphere microorganisms. *Proteomics* **2009**, *9*, 4837–4850.

34. Marmiroli, M.; Pagano, L.; Rossi, R.; Torre-roche, R.D. La; Lepore, G.O.; Ruotolo, R.; Gariani, G.; Bonanni, V.; Pollastri, S.; Puri, A.; *et al*. Copper Oxide Nanomaterial Fate in Plant Tissue: Nanoscale Impacts on Reproductive Tissues. *Environ. Sci. Technol.* **2021**, 10769–10783.

35. Zeng, Y.; Chung, K.P.; Li, B.; Lai, C.M.; Lam, S.K.; Wang, X.; Cui, Y.; Gao, C.; Luo, M.; Wong, K.B.; et al. Unique COPII Component AtSar1a/AtSec23a Pair Is Required for the Distinct Function of Protein ER Export in Arabidopsis Thaliana. *Proc. Natl. Acad. Sci. U. S. A.* **2015**, *112*, 14360–14365.

36. Dangoor, I.; Peled-Zehavi, H.; Levitan, A.; Pasand, O.; Danon, A. A Small Family of Chloroplast Atypical Thioredoxins. *Plant Physiol.* **2009**, *149*, 1240–1250.

37. Sánchez-Fernández, R.; Davies, T.G.E.; Coleman, J.O.D.; Rea, P.A. The Arabidopsis Thaliana ABC Protein Superfamily, a Complete Inventory. *J. Biol. Chem.* **2001**, *276*, 30231–30244.

38. Smith, M.A.; Dauk, M.; Ramadan, H.; Yang, H.; Seamons, L.E.; Haslam, R.P.; Beaudoin, F.; Ramirez-Erosa, I.; Forseille, L. Involvement of Arabidopsis Acyl-Coenzyme A Desaturase-Like2 (At2g31360) in the Biosynthesis of the Very-Long-Chain Monounsaturated Fatty Acid Components of Membrane Lipids. *Plant Physiol.* **2013**, *161*, 81–96.

39. Ruotolo, R.; Maestri, E.; Pagano, L.; Marmiroli, M.; White, J.C.; Marmiroli, N. Plant response to metal-containing engineered nanomaterials: an omics-based perspective. Environ. Sci. Technol. **2018**, 52(5), 2451-2467.

40. Pagano, L.; Marmiroli, M.; Villani, M.; Magnani, J.; Rossi, R.; Zappettini, A.; White, J.C.; Marmiroli, N. Engineered Nanomaterial Exposure Affects Organelle Genetic Material Replication in Arabidopsis Thaliana. *ACS Nano* **2022**, *16*, 2249–2260.

41. Koussevitzky, S.; Stanne, T.M.; Peto, C.A.; Giap, T.; Sjögren, L.L.E.; Zhao, Y.; Clarke, A.K.; Chory, J. An Arabidopsis Thaliana Virescent Mutant Reveals a Role for ClpR1 in Plastid Development. *Plant Mol. Biol.* **2007**, *63*, 85–96.

42. Maiwald, D.; Dietzmann, A.; Jahns, P.; Pesaresi, P.; Joliot, P.; Joliot, A.; Levin, J.Z.; Salamini, F.; Leister, D. Knock-out of the Genes Coding for the Rieske Protein and the ATP-Synthase δ-Subunit of Arabidopsis. Effects on Photosynthesis, Thylakoid Protein Composition, and Nuclear Chloroplast Gene Expression. *Plant Physiol.* **2003**, *133*, 191–202.

43. Wang, Z.; Xu, L.; Zhao, J.; Wang, X.; White, J.C.; Xing, B. CuO Nanoparticle Interaction with Arabidopsis Thaliana: Toxicity, Parent-Progeny Transfer, and Gene Expression. *Environ. Sci. Technol.* **2016**, *50*, 6008–6016.

44. Kuusk, S.; Sohlberg, J.J.; Magnus Eklund, D.; Sundberg, E. Functionally Redundant SHI Family Genes Regulate Arabidopsis Gynoecium Development in a Dose-Dependent Manner. *Plant J.* **2006**, *47*, 99–111.

45. Appelhagen, I.; Huep, G.; Lu, G. H.; Strompen, G.; Weisshaar, B.; Sagasser, M. Weird fingers: functional analysis of WIP domain proteins. *FEBS letters* **2010**, *584*, 3116-3122.

46. Nover, L.; Bharti, K.; Döring, P.; Mishra, S.K.; Ganguli, A.; Scharf, K.D. Arabidopsis and the Heat Stress Transcription Factor World: How Many Heat Stress Transcription Factors Do We Need? *Cell Stress Chaperones* **2001**, *6*, 177–189.

47. Krupinska, K.; Blanco, N.E.; Oetke, S.; Zottini, M. Genome Communication in Plants Mediated by Organelle–Nucleus-Located Proteins. *Philos. Trans. R. Soc. B Biol. Sci.* **2020**, *375*.

48. Akama, K.; Junker, V.; Beier, H. Identification of Two Catalytic Subunits of TRNA Splicing Endonuclease from Arabidopsis Thaliana. *Gene* **2000**, *257*, 177–185.

49. Marmiroli, M.; Imperiale, D.; Pagano, L.; Villani, M.; Zappettini, A.; Marmiroli, N. The proteomic response of *Arabidopsis thaliana* to cadmium sulfide quantum dots, and its correlation with the transcriptomic response. *Front. Plant Sci.* **2015**, *6*, 1104.